

Controlling the Pathway of Photosynthetic Charge Separation in Bacterial Reaction Centers

A. L. M. Haffa,^{†,‡,§} S. Lin,^{†,‡,§} J. C. Williams,^{†,‡} B. P. Bowen,^{†,‡,§} A. K. W. Taguchi,^{†,‡,§}
J. P. Allen,^{†,‡} and N. W. Woodbury^{*,†,‡,§}

Department of Chemistry and Biochemistry, the Center for the Study of Early Events in Photosynthesis, and the Arizona Biodesign Institute, Arizona State University, Tempe, Arizona 85287-1604

Received: July 2, 2003; In Final Form: October 27, 2003

For at least 2 billion years, the structure of the photosynthetic reaction center has maintained an approximate rotational symmetry, in both plants and bacteria, consisting of a heterodimeric core with two ostensibly similar electron-transfer pathways, yet the functional advantage of this symmetry is not clear. This structure/function enigma is nowhere more apparent than in reaction centers isolated from the photosynthetic bacterium *Rhodobacter (Rb.) sphaeroides*. These reaction centers possess two approximately symmetric potential electron transfer pathways (labeled A and B), but stable charge separation is only observed along the A-side in isolated wild type reaction centers. Here we demonstrate that the introduction of two protonatable residues (aspartate and glutamate) in the vicinity of the cofactors involved in initial electron transfer results in pH-dependent switching between A- and B-side charge separation products. At pH 7.2, A-side photochemistry predominates, whereas at pH 9.5, a long-lived B-side charge-separated state is formed almost exclusively. This raises the possibility that a similar control of wild type reaction centers could be mediated either by external factors or by photochemically induced electrostatic changes in vivo.

In *Rhodobacter (Rb.) sphaeroides*, the reaction center consists of three protein subunits and 10 cofactors (Figure 1).^{1,2} Upon excitation of P to form P*, electron transfer along the A-side cofactors occurs in a few picoseconds forming P⁺H_A⁻. A subsequent electron transfer forms P⁺Q_A⁻ in 200 ps. There is essentially no electron transfer along B-side cofactors under these conditions. The difference in function between the two sides must reflect differences in the protein surrounding the chemically identical cofactors (for reviews see refs 3 and 4).

The function of the B-side cofactors in *Rb. sphaeroides* reaction centers is unknown, but the high level of conservation implies that one exists.^{5–7} Excitation directly into the lowest excited singlet states of P, B, or H results in little if any formation of B-side charge-separated states.^{8–17} However, 390 nm excitation results in transient charge separation involving B-side cofactors.¹⁸ The B-side charge-separated state formed is not P⁺H_B⁻, as might be expected in comparison to A-side charge separation, but rather B_B⁺H_B⁻. This state decays within 15 ps at room temperature but is stable for at least hundreds of picoseconds at cryogenic temperatures.

Controlling the Electrostatic Environment with Ionizable Amino Acids. Introducing two acidic amino acid residues in a loop of the L protein subunit at positions within about 10 Å of both P and B_B, results in long-lived B_B⁺H_B⁻ formation upon 390 nm excitation at room temperature.¹⁹ This has been accomplished by changing the histidine at position L168 to glutamic acid and the asparagine at position L170 to aspartic acid, generating the double mutant L168HE/L170ND (Figure 1C).^{20,21} A detailed consideration of the femtosecond spectro-

copy of this mutant and related single and multiple mutants at pH 8.0 has been presented previously.¹⁹

Because the glutamate at L168 and the aspartate at L170 in the mutant are in such close proximity to P and B_B, one would expect that in the ionized form they would have substantial effects on the energetics of any charge-separated states that include either P⁺ or B_B⁺. It is not possible to directly measure the B_B/B_B⁺ midpoint potential because the reaction center denatures at ambient potentials high enough to observe B_B oxidation. However, it is possible to directly measure the P/P⁺ midpoint potential.²⁰ For L168HE/L170ND mutant reaction centers the midpoint potential of P was determined electrochemically at seven pH values between pH 6.0 and 9.5 (data not shown). The effective midpoint potential decreased with increasing pH by about 60 mV over this pH range, with essentially the entire change occurring between pH 6.5 and 8.0. In wild-type reaction centers the P/P⁺ midpoint potential changes by only about 10 mV over the same range of pH values,²⁰ implying that it is the two introduced amino acids that give rise to the bulk of the pH dependence in this mutant. The effect of the two individual mutations on the midpoint potential is approximately additive,²⁰ suggesting that both of the introduced amino acids deprotonate as the pH is increased from pH 6.5 to 9.0. Thus, the introduction of titratable carboxylic acid groups near P and B_B results in a reaction center system with a pH tunable electrostatic environment that affects the energetics of charge-separated states involved in A-side and B-side electron transfer.

Controlling A-Side vs B-Side Charge Separation with pH. The ground-state absorbance spectra of wild type and L168HE/L170ND mutant reaction centers at pH 8.0 are shown in Figure 2. Each of the bacteriochlorophyll and bacteriopheophytin cofactors absorbs in both the Q_x and Q_y regions of the spectrum, and the pathway of electron transfer can be followed by probing

* To whom correspondence should be addressed. E-mail: Nwoodbury@asu.edu.

[†] Department of Chemistry and Biochemistry.

[‡] Center for the Study of Early Events in Photosynthesis.

[§] Arizona Biodesign Institute.

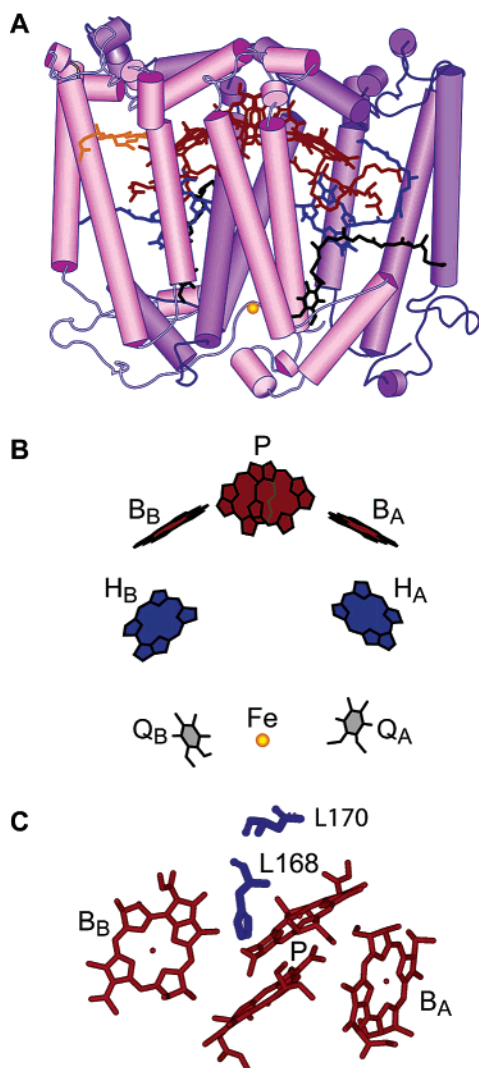


Figure 1. Reaction center structure (A) The L (dark purple) and M (light purple) subunits of the *Rb. sphaeroides* reaction center and associated cofactors (from PDB entry 1PCR). (B) The two sets of cofactors labeled A and B form two potential transmembrane electron-transfer pathways: a bacteriochlorophyll dimer (P), two accessory bacteriochlorophylls B_A and B_B , two bacteriopheophytins H_A and H_B , two quinones Q_A and Q_B , and a non-heme iron (Fe). The sole carotenoid near B_B is shown in panel A but omitted from panel B. (C) The two amino acid residues, L168 (His→Glu) and L170 (Asn→Asp) (blue), that were modified are shown in relationship to P (center), B_A and B_B . The distances from the closest point of the side chain of L168 to the edge of the tetrapyrrole ring of P, B_A , and B_B are 3.0, 13.5, and 3.5 Å, respectively; for L170 the distances are 9.0, 14.5, and 10.5 Å, respectively.

these absorbance bands as a function of time. Time-resolved transient absorbance difference spectra of L168HE/L170ND mutant reaction centers 600 ps after 390 nm excitation at pH 9.5 and 7.2 are shown in Figure 3. (Below pH 7.2 under the conditions of these measurements, the reaction centers were not stable enough for reliable measurements to be performed.) For comparison, spectra showing exclusively A-side charge separation in L168HE/L170ND mutant reaction centers obtained using 850 nm excitation at pH 8.0 are also included.²¹ (Note that 850 nm excitation results in only A-side charge separation in this mutant under all conditions tested, and pH 8.0 data are shown because the best signals were obtained at this pH. Interestingly, at pH 9.5, there is little or no charge separation observed upon direct excitation of P in this mutant, an issue that will be explored in a subsequent publication.)

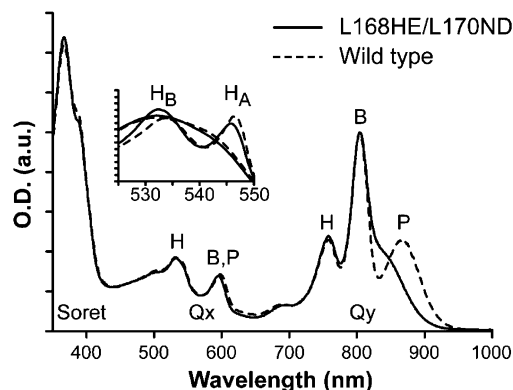


Figure 2. Ground-state absorption spectra. Wild type (dashed line, ---) and L168HE/L170ND (solid line, —) reaction centers at pH 8, room temperature (see Methods). P and the monomer bacteriochlorophylls (B_A and B_B) can be distinguished in the Q_y region of the spectrum, whereas the two bacteriopheophytins (H_A and H_B) can be distinguished in the Q_x region. This is shown more clearly in the inset, which compares spectra taken at 10 K in which the two transitions are clearly resolved with the H_A transition centered at 545 nm and the H_B transition centered at 535 nm. Spectra were also taken at room temperature where these peaks are broader but do not completely overlap and are shifted slightly to the blue such that the H_A transition is centered near 540 nm and the H_B transition is centered near 525 nm.

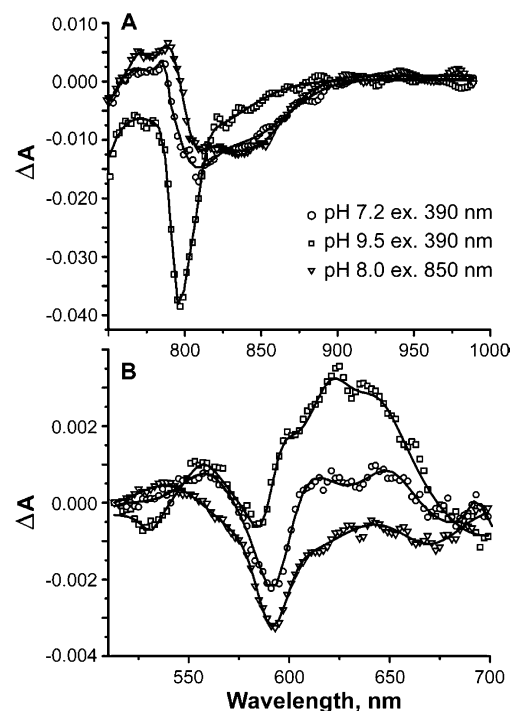


Figure 3. Room-temperature time-resolved transient absorbance difference spectra near 600 ps. (A) Q_y and (B) Q_x spectral region transient absorbance changes for L168HE/L170ND reaction centers at pH 7.2 (circles) and pH 9.5 (squares) following excitation at 390 nm and at pH 8.0 (triangles) following excitation at 850 nm. The state formed using 850 nm excitation at pH 8.0 is $P^+Q_A^-$. At pH 9.5 and 390 nm excitation the state formed is interpreted as exclusively $B_B^+H_B^-$, and at pH 7.2 and 390 nm excitation it is apparently mostly $P^+Q_A^-$ with some $B_B^+H_B^-$ mixed in. See text for details. The lines are fits with an arbitrary number of Lorentzian functions.

The P and B ground-state absorbance bands are clearly distinguished in the Q_y spectral region (Figure 2), and thus this region is used to identify the cation in the transient measurements. In L168HE/L170ND mutant reaction centers at pH 9.5 using 390 nm excitation, an 800 nm bleaching dominates the spectrum and very little bleaching of P is observed (Figure 3A).

This is consistent with the formation of B_B^+ rather than P^+ . In contrast to the situation at pH 9.5, at pH 7.2 a bleaching of the P band and an electrochromic shift of the B band are observed, as would be expected for $P^+Q_A^-$ ²² (Figure 3A). The pH 7.2 spectrum is very similar to that generated in L168HE/L170ND mutant reaction centers by direct excitation of P at 850 nm, which forms the state $P^+Q_A^-$ exclusively²¹ (Figure 3A). The small differences observed between these two transient spectra are probably due to some contribution of $B_B^+H_B^-$ to the pH 7.2 spectrum, as described below. The pH 7.2 difference spectrum near 600 ps is also similar to data recorded for wild type¹⁸ using either excitation at 390 or 860 nm with the exception that the bleaching of the ground-state transition of P is shifted to higher energy in the mutant (Figure 3A).

The Q_x absorbance bands for the two symmetrically related bacteriopheophytins have slightly different transition energies, with H_A absorbing near 540 nm and H_B near 525 nm at room temperature (Figure 2 inset). Thus, by observing the absorbance changes upon charge separation in this region of the spectrum, it is possible to determine whether H_A or H_B is serving as the anion in the charge-separated state formed. Data taken at pH 9.5 in this region (Figure 3B) are characterized by a bleaching near 525 nm due to the loss of the H_B ground-state absorbance band and an absorbance increase due to an anion band of H_B^- centered near 625 nm (the spectrum of the H_B anion has been previously described^{18,23,24}). Little or no bleaching of the H_A ground-state band is observed at 540 nm in Figure 3B, nor is there evidence for a significant contribution of the H_A anion band normally found at 660 nm.^{18,23,24} There is also a bleaching near 580 nm due to the formation of B_B^+ .¹⁸ The combined results from the Q_x and Q_y spectral regions show that 390 nm excitation at pH 9.5 gives rise to almost exclusively $B_B^+H_B^-$ formation on long time scales. At pH 9.5, this state does not decay appreciably on the time scale of the transient absorbance measurements performed (about 1 ns).

Data taken at pH 8.0 using 850 nm excitation (Figure 3B) show a bleaching of the P ground-state transition near 590 nm and relatively flat signals in the regions of the H_A and H_B ground-state transitions (525–540 nm) and the anion absorbance bands (620–670 nm). This is expected because excitation at 850 nm and pH 8.0 gives rise to the state $P^+Q_A^-$ at long times, rather than a state involving bacteriopheophytin. The long-time spectrum taken at pH 7.2 (Figure 3B) also shows a much smaller bleaching of the bacteriopheophytin ground-state band and a much smaller absorbance increase due to anion formation at 625 nm than is observed at pH 9.5. Additionally, the size and position of the 590 nm bleaching is more similar to that observed using 850 nm excitation at pH 8.0 than to the bleaching observed using 390 nm excitation at pH 9.5. However, at pH 7.2, on average one of the two introduced amino acids is likely protonated, and the transient absorbance spectrum does appear to include some $B_B^+H_B^-$ in addition to the $P^+Q_A^-$, though $P^+Q_A^-$ is the dominant species. Of course, $P^+Q_A^-$ can be formed exclusively in this mutant by using 850 nm excitation (Figure 3B). Thus at pH 9.5, 390 nm excitation of L168HE/L170ND mutant reaction centers results in formation of almost exclusively $B_B^+H_B^-$ on long time scales, whereas $P^+Q_A^-$ is formed predominantly at lower pH using 390 nm excitation and exclusively using 850 nm excitation (Figure 4).

Previous measurements have shown that in the wild type, 390 nm excitation results in the formation of a $B_B^+H_B^-$ state with an activated decay, disappearing in picoseconds at room temperature and remaining on the nanosecond time scale at low temperature.¹⁸ Apparently the L168HE and L170ND mutations

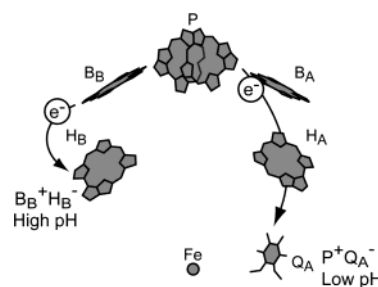


Figure 4. Switching model. The long-lived (>600 ps) charge-separation products formed at pH 9.5 ($B_B^+H_B^-$) and at pH 7.2 ($P^+Q_A^-$) following 390 nm excitation at room temperature. $P^+Q_A^-$ is also formed upon direct excitation of P at 850 nm. Q_B is not shown as it was displaced by 1,10-orthophenanthroline for these studies.

raise the activation barrier for decay of $B_B^+H_B^-$, but only at high pH where the introduced carboxylic acid residues are in the charged form. Presumably, this is either due to the stabilization of B_B^+ by the negative charges or due to destabilization of the activated decay intermediate.

The symmetric structure of the reaction center provides a unique opportunity to study in detail the role of the protein environment in mediating electron transfer reactions. In isolated wild type reaction centers, only A-side cofactors are involved in charge-separated states that persist on the nanosecond time scale at room temperature. It has been shown here that simply by altering the local electrostatics through changes in the ionization state of two genetically introduced acidic residues, the identity of the long-lived photochemical product formed can be switched between a charge-separated state involving predominantly A-side cofactors and one involving almost exclusively B-side cofactors. It may be that in wild-type reaction centers in vivo, interactions with other cellular components or photochemically induced charge separated states are able to regulate the electrostatic environment, mimicking the switching capabilities of the L168HE/L170ND mutant. In addition to the possible biological implications of this, such a system also represents an interesting model for a molecular electronic switch in which both wavelength and pH can be used to control the pathway of electron transfer on a molecular scale.

Methods

Reaction Center Isolation and Midpoint Potential Determination. L168HE/L170ND reaction centers were isolated^{20,21} and suspended in TLE [15 mM tris(hydroxymethyl)aminomethane–HCl (Tris–HCl), 0.025% lauryldimethylamine *N*-oxide (LDAO), 1 mM (ethylenediamine)tetraacetic acid (EDTA), pH 8.0 or 7.2], or CLE [15 mM 2-(cyclohexylamino)ethanesulfonic acid (CHES), 0.025% LDAO, 1 mM EDTA, pH 9.5] for all spectroscopic studies. Midpoint potential measurements were performed electrochemically as described previously.²⁰ In the pH range from 7.5 to 8.5, reaction centers were in 15 mM Tris–HCl, 0.01% Triton X-100, and 1 mM EDTA. The buffer was changed to 15 mM 2-(*N*-morpholine)ethanesulfonic acid for measurements from pH 6.0 to 7.0, and 15 mM CHES for measurements from pH 9.0 to 9.5.

Femtosecond Transient Absorbance Measurements. The reaction center preparation²¹ and the apparatus used for subpicosecond transient absorption spectroscopy have been described.^{18,25} Buffer conditions are described above. 1,10-Orthophenanthroline was added to block electron transfer to Q_B . Ultrafast laser pulses (100 fs duration) at 390 nm and at 850 nm were used to excite the reaction center Soret band and the Q_y transition of P, respectively. Room-temperature data

were collected from 480 to 1025 nm (two sets of data from 480 to 780 and 730–1025 nm were acquired) as previously described.^{25–27}

References and Notes

- (1) Allen, J. P.; Feher, G.; Yeates, T. O.; Komiya, H.; Rees, D. C. *Proc. Natl. Acad. Sci. U.S.A.* **1987**, *84*, 5730–5734.
- (2) Allen, J. P.; Feher, G.; Yeates, T. O.; Komiya, H.; Rees, D. C. *Proc. Natl. Acad. Sci. U.S.A.* **1988**, *85*, 8487–8491.
- (3) Gunner, M. *Curr. Top. Bioenerg.* **1991**, *16*, 319–367.
- (4) Allen, J. P.; Williams, J. C. *Bioenerg. Biomembr.* **1995**, *27*, 275–283.
- (5) Schubert, W. D.; Klukas, O.; Saenger, W.; Witt, H. T.; Fromme, P.; Krauss, N. *J. Mol. Biol.* **1998**, *280*, 297–314.
- (6) Blankenship, R. E. *Trends Plant Sci.* **2001**, *6*, 4–6.
- (7) Barber, J. *Q. Rev. Biophys.* **2003**, *36*, 71–89.
- (8) Kirmaier, C.; Holten, D.; Parson, W. W. *Biochim. Biophys. Acta* **1985**, *810*, 49–61.
- (9) Kirmaier, C.; Holten, D.; Parson, W. W. *Biochim. Biophys. Acta* **1985**, *810*, 33–48.
- (10) Breton, J.; Martin, J.-L.; Migus, A.; Antonetti, A.; Orszag, A. Femtosecond spectroscopy of excitation energy transfer and initial charge separation in the reaction center of the photosynthetic bacterium *Rhodospseudomonas sphaeroides*. *Ultrafast Phenomena V*, 1986.
- (11) Martin, J.-L.; Vos, M. H. *Annu. Rev. Biophys. Biomol. Struct.* **1992**, *21*, 199–222.
- (12) Kirmaier, C.; Holten, D. Electron transfer and charge recombination reactions in wild-type and mutant bacterial reaction centers. In *The Photosynthetic Reaction Center*; Deisenhofer, J., Norris, J. R., Eds.; Academic Press: San Diego, 1993; Vol. II, pp 49–70.
- (13) Ermler, U.; Fritzsche, G.; Buchanan, S. K.; Michel, H. *Structure* **1994**, *2*, 925–936.
- (14) Walker, G. C.; Maiti, S.; Reid, G. D.; Wynne, K.; Moser, C. C.; Pippenger, R. S.; Cowen, B. R.; Dutton, P. L.; Hochstrasser, R. M. Femtosecond infrared spectroscopy of the photosynthetic reaction center. *Ultrafast Phenomena IX*, 1994, Berlin, Heidelberg.
- (15) Jia, Y.; Jonas, D. M.; Joo, T.; Nagasawa, Y.; Lang, M. J.; Fleming, G. R. *J. Phys. Chem.* **1995**, *99*, 6263–6266.
- (16) Lancaster, C. R. D.; Ermler, U.; Michel, H. The structure of photosynthetic reaction centers from purple bacteria as revealed by X-ray crystallography. In *Anoxygenic Photosynthetic Bacteria*; Blankenship, R. E., Madigan, M. T., Bauer, C. E., Eds.; Kluwer Academic Publishers: Dordrecht, The Netherlands, 1995; Vol. 2; pp 503–526.
- (17) Parson, W. W. Photosynthetic bacterial reaction centres. In *Protein Electron Transfer*; Bendall, S. D., Ed.; BIOS Scientific Publishers: Oxford, U.K., 1996; pp 125–160.
- (18) Lin, S.; Katilius, E.; Haffa, A. L. M.; Taguchi, A. K. W.; Woodbury, N. W. *Biochemistry* **2001**, *40*, 13767–13773.
- (19) Haffa, A. L. M.; Lin, S.; Williams, J. C.; Taguchi, A. K. W.; Allen, J. P.; Woodbury, N. W. *J. Phys. Chem B*, in press.
- (20) Williams, J. C.; Haffa, A. L. M.; McCulley, J. L.; Woodbury, N. W.; Allen, J. P. *Biochemistry* **2001**, *40*, 15403–15407.
- (21) Haffa, A. L. M.; Lin, S.; Katilius, E.; Williams, J. C.; Taguchi, A. K. W.; Allen, J. P.; Woodbury, N. W. *J. Phys. Chem. B* **2002**, *106*, 7376–7384.
- (22) Woodbury, N.; Allen, J. P. Electron Transfer in Purple Nonsulfur Bacteria. In *Anoxygenic Photosynthetic Bacteria*; Blankenship, R. E., Madigan, M. T., Bauer, C. E., Eds.; Kluwer: Boston, 1995; Vol. 2, pp 527–557.
- (23) Robert, B.; Lutz, M.; Tiede, D. M. *FEBS Lett.* **1985**, *183*, 326–330.
- (24) Heller, B. A.; Holten, D.; Kirmaier, C. *Science* **1995**, *269*, 940–945.
- (25) Freiberg, A.; Timpmann, K.; Ruus, R.; Woodbury, N. W. *J. Phys. Chem. B* **1999**, *103*, 10032–10041.
- (26) Greene, B. I.; Farrow, R. C. *Chem. Phys. Lett.* **1983**, *98*, 273–276.
- (27) Katilius, E.; Turanchik, T.; Lin, S.; Taguchi, A. K. W.; Woodbury, N. W. *J. Phys. Chem. B* **1999**, *103*, 7386–7389.